Hysteresis in Superconducting Alloys—Temperature and Field Dependence of Dislocation Pinning in Niobium Alloys*

W. A. FIETZ† AND W. W. WEBB
Department of Applied Physics and Laboratory of Atomic and Solid State Physics, Cornell University, Ithaca, New York 14850

(Received 9 September 1968)

Critical current and pinning-force densities in a series of niobium alloys subjected to severe plastic deformation have been determined from measurements of complete hysteretic magnetization curves on alloys with Ginzburg-Landau parameter κ between 1.3 and 13 at temperatures from the critical temperature T_c down to $0.14T_c$. Systematic scaling rules were found that accurately describe all of the results over the entire range of fields and temperatures. The pinning-force density scales with magnetic induction as a single function of B/H_{c2}; it scales with temperature as the $\frac{5}{2}$ power of the upper critical field $H_{c2}(T)$, is roughly proportional to $\kappa^{-\gamma}$, where $1<\gamma<3$, and is otherwise independent of T. A model for the pinning process that takes into account deformation of the fluxoid lattice by the pinning forces is proposed to account for the observed scaling rules. The results are consistent with a pinning interaction based on a second-order elastic interaction between dislocations and the fluxoid lattice, but other mechanisms are not excluded. Cooperative effects seem to be an essential feature of the pinning process, leading to a dependence of the pinning-force density on the square of the pinning-point strength, and on the arrangement of pinning points.

I. INTRODUCTION

THE concept of the critical state introduced by Bean[1] and developed by Kim *et al.*[2,3] and by Anderson[4] provides a phenomenological theory of magnetic hysteresis in type-II superconductors in magnetic fields between the onset of flux penetration and the upper bulk critical field H_{c2}. The critical state describes a current distribution throughout the superconductor that is supposed to be determined by the effectiveness of material inhomogeneities in pinning a flux distribution against Lorentz forces. Kim's analysis with de Gennes's[5] thermodynamic definition of forces appears to provide a satisfactory basis for describing experimental results on most magnetic hysteresis and transport currents in high-field superconductors. In low κ materials, additional hysteretic surface currents may also appear, presenting an experimental difficulty in separating surface and bulk effects. This paper deals only with cases in which bulk hysteresis dominates.

The measured dependence of critical current density J_c on local magnetic induction B has often been described by some convenient empirical formula. However, simple formulas for $J_c(B)$ used in model calculations have sometimes been erroneously regarded as inherent properties of the critical state. In fact, we are aware of only one detailed theory[6] that attempts to calculate $J_c(B)$ due to an assembly of pinning points for a wide range of B.

Therefore, the objective of this research was to obtain experimental data on $J_c(B)$ for a wide range of κ and T on a particular type of pinning structure in order to provide a guide and a test for theoretical studies.

Several phenomenological calculations of the strength of the interaction between individual fluxoids and particular kinds of pinning points are available. Silcox and Rollins[7] and Friedel *et al.*[8] have calculated the effects of pinning of a very dilute fluxoid lattice by cavities and Webb[9] and Cramer and Bauer[10] have calculated the interaction between a single fluxoid and the strain field of a screw dislocation. Labusch[11] has recently established a thermodynamic basis for calculations of pinning a fluxoid by a strain field. Willis *et al.*[12] have recently calculated the strength of pinning due to a region of disparate κ.

Clear experimental verification of critical-state concepts has been obtained for various type-II superconductors.[2,3,10] However, there is a large body of experimental data (see review by Livingston and Shadler[13]) very little of which is amenable to quantitative analysis. Nembach[14] has reported a value of the pinning strength of dislocations derived from remanent (trapped) flux measurements at 4.2°K in plastically deformed niobium. However, it is unfortunately somewhat doubtful because of the uncertain distribution of internal magnetic

* Research supported by the U. S. Atomic Energy Commission and benefitted from facilities provided by the Advanced Research Projects Agency at Cornell University.

† Present address: Linde Division, Union Carbide Corp., Indianapolis, Ind.

[1] C. P. Bean, Phys. Rev. Letters **8**, 250 (1962).

[2] Y. B. Kim, C. F. Hempstead, and A. R. Strnad, Phys. Rev. Letters **9**, 306 (1962).

[3] Y. B. Kim, C. F. Hempstead, and A. R. Strnad, Phys. Rev. **129**, 528 (1963).

[4] P. W. Anderson, Phys. Rev. Letters **9**, 309 (1962); Rev. Mod. Phys. **36**, 39 (1964).

[5] P. G. de Gennes, *Superconductivity of Metals and Alloys* (W. A. Benjamin, Inc., New York 1966), Chap. 3.

[6] R. Labusch (private communication).

[7] J. Silcox and R. W. Rollins, Appl. Phys. Letters **2**, 321 (1963).

[8] J. Friedel, P. G. de Gennes, and J. Matricon, Appl. Phys. Letters **2**, 119 (1963).

[9] W. W. Webb, Phys. Rev. Letters **11**, 191 (1963).

[10] E. J. Cramer and C. L. Bauer, Phil. Mag. **15**, 1189 (1967).

[11] R. Labusch, Phys. Rev. **170**, 470 (1968).

[12] J. S. Willis, J. F. Schenck, and R. W. Shaw, Appl. Phys. Letters **10**, 101 (1967).

[13] J. D. Livingston and H. W. Schadler, Progr. Mater. Sci. **12**, 183 (1964).

[14] E. Nembach, Phys. Status Solidi **13**, 543 (1966).

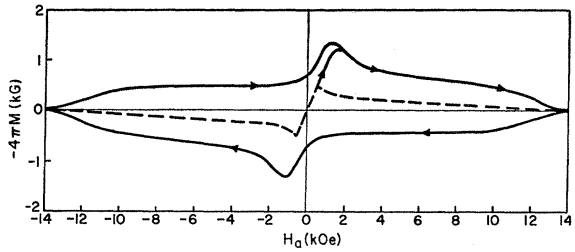

FIG. 1. Typical hysteretic magnetization curve obtained by electronic integration. Data apply to Nb+4 at.% Ti alloy at 4.2°K. The reversible curve for the same material after annealing is also shown as a dashed line for comparison. Data for M_e and $dH_e(B)/dB$ were taken from the reversible curve.

fields in this measurement. Narlikar and Dew-Hughes[15] have reported quantitative data comparing various treatments of deformed niobium alloys. Fietz *et al.*[16] have derived rather precise values of critical-state pinning-force densities from magnetization and transport current measurements at 4.2°K but the materials studied were commercially treated alloys of niobium-25 at.% zirconium that contain a complex mixture of metallurgical inhomogeneities. Coffey[17] has reported measurements of the field and temperature dependence of the critical current density in heat-treated niobium alloys and Freyhardt and Haasen[18] have recently reported magnetization measurements on lightly cold-worked niobium single crystals that have been interpreted to indicate a pinning force of 10^{-7} dyn for individual dislocation-fluxoid interactions.

This paper reports in detail experimental values of the critical-current density J_c and pinning-force density F_p due to dislocation pinning over a wide range of temperature and magnetic field. These quantities were measured on a series of heavily cold-worked niobium-titanium and niobium-tantalum alloys, in which the Ginzburg-Landau parameter κ varied from about 1.3 to 13. In most of these alloys it was possible to vary the temperature T between about $0.14T_c$ and T_c, and the magnetic induction B from about $0.1H_{c2}$ to H_{c2}. The data thus obtained were found to be highly reproducible, and a set of remarkably consistent scaling rules was found. The results are compatible with critical-state concepts, and at least one simple pinning model. A model suggested by a theory of Labusch[6] has been invoked to take into account cooperative effects in the fluxoid lattice in making connection between the measured pinning-force density and individual pinning point interactions. A preliminary report of some of the experimental results has been given by Webb and Fietz.[19]

[15] A. V. Narlikar and D. Dew-Hughes, J. Mater. Sci. **1**, 317 (1966).
[16] W. A. Fietz, M. R. Beasley, J. Silcox, and W. W. Webb, Phys. Rev. **136**, A335 (1964).
[17] H. T. Coffey, Phys. Rev. **166**, 447 (1968).
[18] H. Freyhardt and P. Haasen, Z. K. Metall. **58**, 856 (1967).
[19] W. W. Webb and W. A. Fietz, in *Proceedings of the Tenth International Conference on Low Temperature Physics, Moscow, 1966*, edited by M. P. Malkov (Proizvodstrenno-Izdatel'skii Kombinat, VINITI, Moscow, 1967), Vol. II B, p. 21.

II. EXPERIMENTAL

Data for the critical current and pinning-forces densities were derived from magnetization curves on long cylindrical specimens cycled in a longitudinal applied field using an analysis described in the Appendix. The curves were obtained by electronic integration[20] of the difference in terminal voltage of two identical balanced coils, one of which contained the specimen as the applied field was slowly varied. This voltage, proportional to the magnetic moment, was plotted on the Y axis of an X-Y recorder with a voltage proportional to the applied field H, obtained by integrating the output of the empty coil, plotted on the X axis. Calibration of the vertical axis in terms of average magnetization was carried out by making use of the initial diamagnetic slope obtained after the specimen was cooled in zero field. A typical curve is shown in Fig. 1 along with the reversible curve obtained from an annealed specimen of the same alloy composition. A detailed study of the reversible behavior of the annealed alloys has been published elsewhere.[21]

The applied field was provided by a 40-kOe solenoid powered by a self-ramping current regulator.[22] The field was uniform to 0.05% over a distance of about 6 cm in a bore of 3.8-cm diam.

In order to provide temperature adjustment over the range between 1.2 and 15°K, the specimen and coil assembly were mounted in a vacuum-insulated can inserted within the bore of the solenoid. Temperatures below 4.2°K were obtained by varying the vapor pressure above liquid helium in which the specimen was immersed. Manostat control held temperature fluctuations to less than 0.01°K under these conditions. Temperatures above 4.2°K were obtained by electrically heating a brass wire coil within the specimen chamber in the presence of helium gas at about 1 Torr. Temperatures were measured with a carbon resistor in thermal contact with the specimen. This resistor was also used in a feedback system to control the temperature during the heating. Temperature fluctuations above 4.2°K were less than 0.1°K, and were mainly due to magnetoresistance of the carbon resistor that was not compensated.

The alloys were prepared under the supervision of Professor J. L. Gregg of the Materials Science Center Metallurgical Facility at Cornell University by arc melting high-purity materials which had previously been electron beam zone refined. Chemical analysis of these specimens is given in Table I.

After multiple arc melting in an argon atmosphere with particular care to ensure purity and uniformity, the specimens were swaged from the original 1.25-cm ingots to 0.37-cm diam without intermediate anneal. A chemical polish to 0.36-cm diam was found to be sufficient to

[20] W. A. Fietz, Rev. Sci. Instr. **36**, 1621 (1965).
[21] W. A. Fietz and W. W. Webb, Phys. Rev. **161**, 423 (1967).
[22] W. A. Fietz, Rev. Sci. Instr. **36**, 1306 (1965).

remove the heavy surface damage, and we think that magnetization curves obtained from the specimens thus prepared are representative of uniform flux pinning throughout the specimens, since a further decrease in size produced no more change in the deduced values of critical current density.

The severe plastic deformation produced by swaging to a reduction of cross-sectional area by a factor greater than 11 without intermediate annealing is expected to produce a macroscopically uniform distribution of dislocations at a density of about 10^{11} per cm^2 in all these alloys. Such structures are known from electron-microscopy studies to consist of cells less than 1 μ across that are nearly free of dislocations, but are bounded by quite diffuse cell walls of dense dislocation tangles. Recently, the dislocation structure of deformed niobium has been studied in detail by Christian *et al.*[23] No isolated slip bands or macroscopic undeformed regions would remain following the extremely heavy plastic deformation that was used in our preparation.

The approximate equilibrium magnetization of these materials was obtained from data on carefully annealed specimens of identical composition. The changes in equilibrium properties, such as H_{c2}, due to cold working were small in the alloys reported here.

Resistivity and resistivity ratios were obtained by measuring the voltage drop along the specimen in the presence of a transport current at room temperature and at 4.2°K in a field sufficient to quench superconductivity or in one case at a temperature slightly above the critical temperature.

III. PARAMETERS OF CRITICAL-STATE THEORY

In a type-II superconductor, de Gennes[5] has shown that it is possible to define, for a nonequilibrium flux distribution within the material, a force density equal to the gradient of the magnetic pressure. This force tends to even out the internal flux distribution and thus reduce internal current densities. The expression given by de Gennes is

$$F=(B/4\pi)(dB/dx)[dH_e(B)/dB], \quad \text{(Gaussian units)} \quad (1)$$

or in customary form,

$$F=(JB/10)[dH_e(B)/dB], \quad \text{(practical units)}$$

where $H_e(B)$ is the external applied field which would produce the equilibrium magnetic induction B within the material if there were no flux pinning whatever. These equations apply to a virtually infinite-length flat plate or a cylindrical geometry with applied field parallel to the surface in which lines of flux remain essentially straight. The second equation gives the volume force in dynes per cubic centimeter if B is in gauss and J is in amperes per square centimeter.

[23] J. Christian *et al.*, Phil. Mag. **15**, 873 (1967); **15**, 893 (1967).

TABLE I. Chemical analysis of cold-worked niobium-based alloys.

Nominal composition (at.%)	Actual composition (at.%)	Carbon (ppm)	Oxygen (ppm)	Tantalum (ppm)	Other metals (ppm)
Nb-5 Ta	Nb-5.3 Ta	...	...	...	...
Nb-1.5 Ti	Nb-1.5 Ti				
Nb-2 Ti	Nb-1.9 Ti	120–155[a]	80–200[a]	100–250[a]	10–50[a]
Nb-4.5 Ti	Nb-4.2 Ti				
Nb-4.5 Ti	Nb-3.6 Ti				
Nb-9 Ti	Nb-9.1 Ti				
Nb-12 Ti	Nb-11.7 Ti				

[a] Range observed in tests of six different specimens selected from this group.

In the steady state the force density is supposed to be balanced by forces representing the resistance to motion of fluxoids through the superconductor. The critical state is defined by the limiting current density J_c at which the fluxoid array is essentially stationary. Thus a specimen is said to be in the critical state if the force density F due to the gradient of the magnetic pressure is everywhere equal to the maximum of a resistance to passage (at infinitesimal velocity) of the fluxoid array due to inhomogeneities in the superconductor. This resistance which presumably depends on local magnetic field B, temperature T, and, of course, the microstructure and composition of the material, is called the pinning-force density F_p.

Anderson[4] advanced the concept of flux creep to describe the motion of the vortices where thermal activation processes might be important. In this theory the flux bundle is a simple way to incorporate collective effects that result from the long range of interaction between the fluxoids that make it difficult to move or to pin a single fluxoid without affecting a substantial number of neighbors. The flux-creep model assumes that the rate at which flux bundles escape a pinning barrier can be expressed in terms of an activation energy U and a rate R_0 as

$$R=R_0\exp(-U/k_BT), \quad (2)$$

where k_B is Boltzmann's constant. The activation energy U for a flux bundle may be written

$$U=U_p-V_pFX_p, \quad (3)$$

where U_p is the energy barrier for bundle motion, V_p is the bundle volume, F is the gradient of the magnetic pressure described by de Gennes, and X_p is some characteristic length relating the force to an energy. The concept of the critical state at nonzero temperatures in the presence of flux creep depends on the condition that during the measurements the rate of flux creep is sufficiently small that it has a negligible effect. If the creep rate is designated as R_c, Eqs. (1) and (2) may be combined to give Anderson's result in modified notation:

$$F_c=[U_p-k_BT\ln(R_0/R_c)](X_pV_p)^{-1}. \quad (4)$$

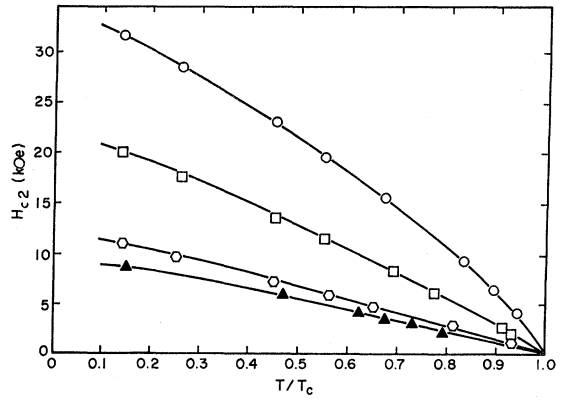

FIG. 2. Upper critical field H_{c2} as a function of reduced temperature for the four alloy compositions studied in detail. Alloy solutes are 5 Ta, 1.5 Ti, 4.5 Ti, and 9 Ti at.%, respectively, from the bottom to the top curve.

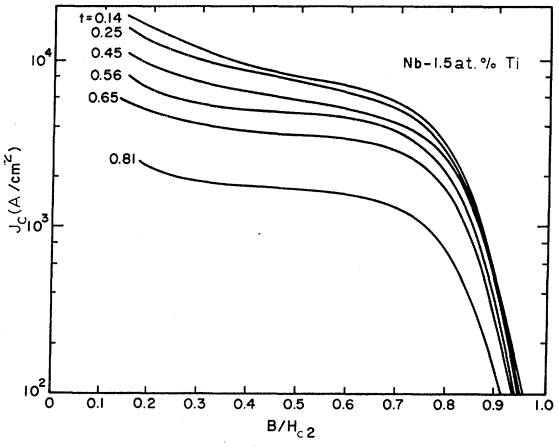

FIG. 4. Logarithmic plot of the critical current density versus reduced field for Nb-1.5 at.% Ti.

If the details of the interactions involved in the pinning of these flux bundles and the type and distribution of the pinning sites were known, the quantities in Eq. (4) could be calculated and a relationship for the measurable quantity F_c could be obtained as a function of local field and temperature and of the pinning parameters. Lacking this, one may seek to deduce the parameters X_p and U_p from the experimental data.

Even assuming that these three parameters are appropriate, they cannot each be fully determined from a critical current experiment without further assumptions about their dependence on T and B. Thus a strategy of seeking reasonable elementary alternatives for comparison with experiment will be adopted for discussion of the dependence of F_c on T, B, and κ.

It is convenient to express some of the temperature dependence in terms of the temperature dependence of the fundamental superconducting parameters $H_c(T)$ and κ through the temperature dependence of $H_{c2}(T) = \sqrt{2}\kappa H_c(T)$, which is easily measured.

The explicitly linear temperature dependence of the second term on the right-hand side of Eq. (4) turns out to be negligible because $k_B T \ln(R_0/R_c) \ll U_p$. Under this condition $F_c \approx F_p$ and the pinning-force density is determined. In anticipation of this result, F_p is substituted for F_c in subsequent discussions of pinning and the two quantities are used interchangeably except where the distinction is explicitly involved.

IV. RESULTS

In this section we present the experimental results as plots of pinning-force density F_p and critical-current density J_c obtained from measured magnetization curves using the equations derived in the Appendix. To illustrate the field and temperature dependence of the volume pinning force F_p, the behavior of four specimens, alloy compositions Nb-5 at.% Ta, Nb-1.5 at.% Ti, Nb-4.5 at.% Ti, and Nb-9 at.% Ti, are presented in detail in forms involving only the assumption of generally homogeneous pinning-force density and the exist-

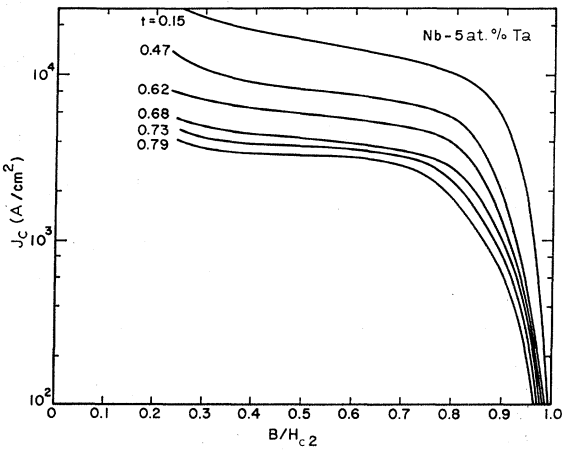

FIG. 3. Logarithmic plot of the critical current density versus reduced field for Nb-5 at.% Ta.

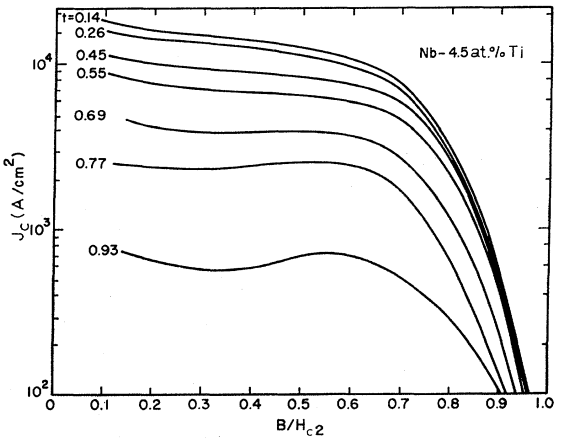

FIG. 5. Logarithmic plot of the critical current density versus reduced field for Nb-4.5 at.% Ti.

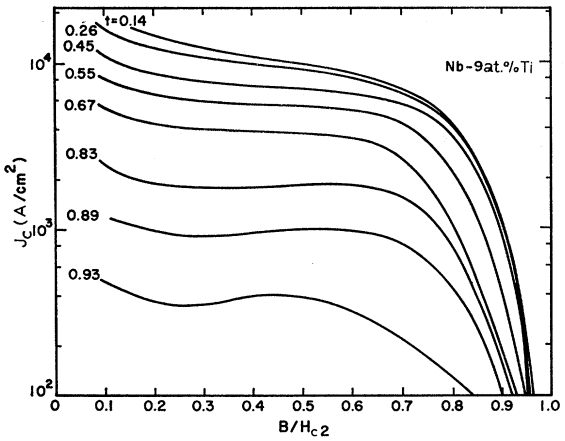

FIG. 6. Logarithmic plot of the critical current density versus reduced field for Nb-9 at.% Ti.

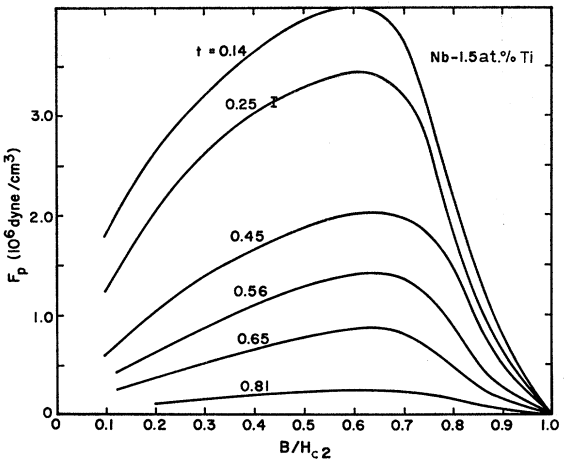

FIG. 8. Pinning-force density for Nb-1.5 at.% Ti.

ence of a bulk-current density determined by Maxwell's equations. These results, which are typical of a larger number of specimens studied, represent a wide range of the Ginzburg-Landau parameter κ. A summary including some additional data is displayed in a later figure.

In Fig. 2, the upper critical field H_{c2} is displayed as a function of temperature for the four specimens whose behavior is to be considered in detail since H_{c2} is an important parameter in the analysis. These data were taken directly from the magnetization curves. The estimated over-all uncertainty which is smaller than the size of the points is due mostly to the slight smearing of the magnetic transition at H_{c2}. Since H_{c2} is altered only slightly by plastic deformation of these alloys, the values of $-4\pi M_e(H)$ and $\gamma=dH_e(B)/dB$ required to calculate J_c and F_p could be obtained directly from measurements of the nearly reversible magnetization of annealed specimens of compositions identical to the plastically deformed alloys.

Using the relationships derived in the Appendix, the critical current densities have been obtained from the magnetization data as a function of temperature and local magnetic induction B. These results are shown in Figs. 3–6, where the logarithm of the critical current density J_c is plotted as a function of the reduced local field B/H_{c2}, at temperatures given as reduced temperature $t=T/T_c$. Data points are not shown since the curves are derived from continuous magnetization curves, and calculations were performed at a sufficient number of points that interpolative error is negligible. The error bar represents the estimated over-all uncertainty in the measurement. The results in this form show the plateau commonly exhibited by the current density in hard superconductors at $t\ll 1$. At higher temperatures they show a broad range in which the critical current falls gradually with increasing B. The sharp increase in J_c that occurs as $B\rightarrow 0$ in measurements of critical transport currents is not accessible in these experiments.

Figures 7–10 present values of the critical Lorentz force density as defined by Eq. (1) and equated with the pinning-force density F_p plotted as functions of the normalized parameter B/H_{c2} for the same measurements used in Figs. 2–6. In every case the presence of a

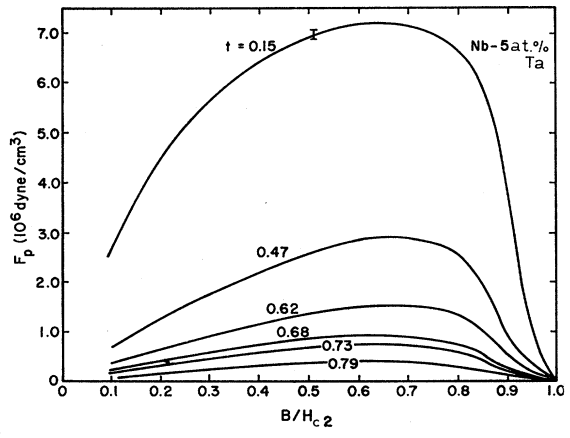

FIG. 7. Pinning-force density as calculated using Eq. (1) plotted as a function of normalized magnetic field for Nb-5 at.% Ta.

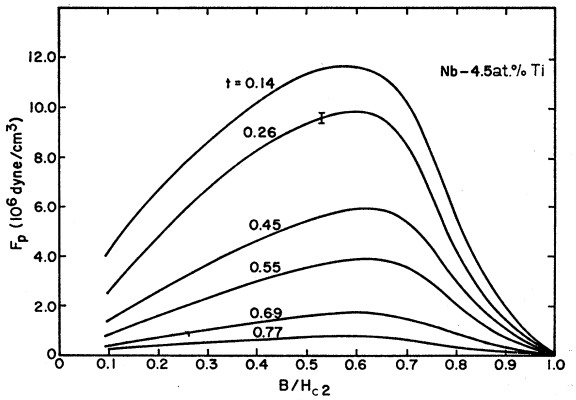

FIG. 9. Pinning-force density for Nb-4.5 at.% Ti.

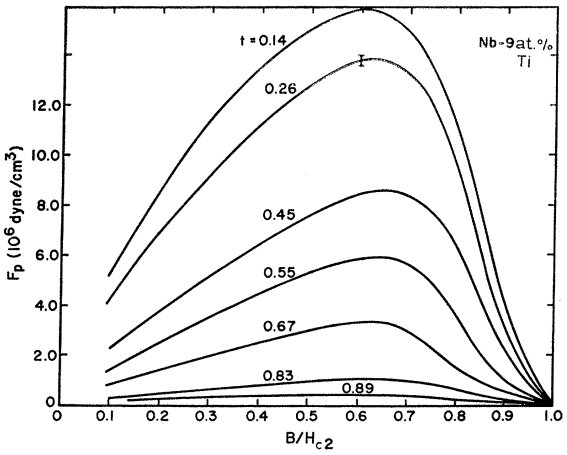

FIG. 10. Pinning-force density for Nb-9 at.% Ti.

maximum of the pinning-force density around B/H_{c2} $\sim$0.6 is evident. The decline of F_p at higher fields and temperatures is clear in these results.

Figure 11 shows a logarithmic plot of the maximum value of F_p obtained at each temperature as a function of H_{c2} at that temperature for each of seven specimens. The temperature range is approximately the same for each alloy. The straight lines are drawn with a slope of $\frac{5}{2}$.

V. DISCUSSION

Discussion of our experiments proceeds in two phases. First, we examine the results with a minimum of theoretical prejudice to discover and identify any general properties or scaling rules. Second, we proceed in a more speculative vein to introduce a model for the critical pinning-force density due to an array of pinning points, consider its properties and the possible pinning mechanisms, and compare the results with the experimental scaling rules.

The two independent experimental parameters are of course magnetic field H or better, internal field B, and the temperature T. We look for scaling laws for the dependence of the pinning force F_p on these quantities. The properties of the superconducting material may be described in Ginzburg-Landau theory by a pair of parameters such as the critical field $H_c(T)$ representative of the condensation energy $[H_c(T)]^2/8\pi$ and the dimensionless, nominally temperature-independent Ginzburg-Landau parameter κ. In the alloy system studied, $H_c(T)$ is practically independent of composition and the generalized Ginzburg-Landau perameters κ_1 and κ_2 show a strong temperature dependence. Fortunately, it turns out that $H_{c2}(T)=\sqrt{2}\kappa_1(T)H_c(T)$ is the appropriate parameter to scale both the temperature and the magnetic field. Pinning introduces additional scaling parameters including the density and distribution of pinning points which were not varied in this series of experiments. The properties of the pinning points themselves suggest the fundamental superconducting lengths $\xi(T)$ the coherence length and $\lambda(T)$ penetration depth as appropriate parameters to compare with the characteristic width of the pinning points and with the nominal fluxoid spacing $d=(\varphi_0/B)^{1/2}$.

The results of analysis of the field dependence have been anticipated by the data presentation in Figs. 3–10. The similarity of the curves generated by plotting F_p in Figs. 7–10 as functions of the field B scaled by H_{c2} identifies a scaling parameter H_{c2}. Each curve has a maximum at $B/H_{c2}(T)=0.6$ within the experimental uncertainty of ± 0.1, a concave upward portion near H_{c2}, and a nearly straight or slightly concave downward portion at low fields. In fact all of the data can be superimposed by appropriate linear scaling of F_p by plotting against B/H_{c2}, except possibly at the lowest fields, where the data analysis begins to fail.

Examination of the scaling of F_p with various parameters leads to the remarkable result illustrated in Fig. 11. Here the logarithm of the maximum value of $F_p(T)$ at each temperature of measurement is plotted against the corresponding logarithm of $H_{c2}(T)$ for each alloy. We see that in each case a straight line with the slope $\frac{5}{2}$ fits the data well within the expected experimental error. The data determine these slopes to be 2.5 ± 0.1. Similar results are obtained on choosing the values of F_p at other values of B/H_{c2}, although the scatter is increased. All of the alloys studied showed this same characteristic scaling of F_p with H_{c2}; thus the straight lines drawn through the data are parallel.

The dependence of F_p on alloy composition is not so precisely determined because the deformation produced in each specimen may not be identical. However, duplicate specimens were identical in behavior as illustrated by the data on two specimens with nominal composition 4.5-at.% titanium included in Fig. 11. These two specimens were melted in different runs and were worked at different times. The specimen labeled 6-at.% titanium is known to be detectably nonuniform and somewhat contaminated; nevertheless, the same temperature dependence prevails. Thus the temperature scaling with $H_{c2}^{5/2}$ seems to be insensitive to vagaries of specimen preparation. All of our data on $F_{p(\max)}$ in the high-purity alloys scale with $\kappa^{-\gamma}$, where $1<\gamma<3$. $F_{p(\max)}$ in the dirtier alloys also decreases as κ increases.

The field dependence of F_p does not fit a simple polynomial in $X\equiv B/H_{c2}$ but the form $X^n(1-X)^m$ has previously been used[15] as a convenient empirical fit in the range $0.1<X<0.9$ with $n=\frac{1}{2}$ and $m=1$. Near $H_{c2}F_p\propto 1-X$ as $X\rightarrow 1$ and at low fields $F_p\propto X$ or $X^{1/2}$ as $X\rightarrow 0$ provide better limiting forms but these factors combined do not reproduce the clearly observed maxima of F_p at $X=0.6$. Coffey[17] has observed rather similar field and temperature dependence in severely cold-worked commercial niobium-titanium and niobium-zirconium alloys.

The scaling rules thus assume the product form

$$F_p=Kk(\kappa)g(B/H_{c2})[H_{c2}(T)]^{5/2}, \qquad (5)$$

where the function $g(B/H_{c2})$ is illustrated by Figs. 7–10 and $k(\kappa)$ is something like $\kappa^{-\gamma}$, with $1<\gamma<3$. The factor $[H_{c2}(T)]^{5/2}$ is established with high precision, $g(B/H_{c2})$ and K are determined to better than $\pm 15\%$ for $0.2<B/H_{c2}<0.9$, but $k(\kappa)=\kappa^{-\gamma}$ is only a qualitative form.

VI. PINNING MODEL

Our results give a systematic description of the pinning-force density in the particular case of a very high density of dislocations from which we might hope to deduce some information about the properties of the pinning points and thus the mechanism responsible for pinning of the fluxoid lattice by dislocations. There are about six distinct mechanisms, all of which are expected to provide $\sim 10^{-8}$ dyn for each dislocation-fluxoid interaction in the low-temperature limit. However, there is an intervening difficulty that has commonly been ignored. This is the need for a satisfactory theory connecting the measured continuum quantity F_p and the array of local interactions f_p between dislocations and fluxoids that sum to F_p. Although no satisfactory theory for this problem has yet been published, our discussion is based on an empirical approach that we hope provides a beginning. It anticipates and is consistent with a forthcoming detailed theory due to Labusch.[6] The final form of both is similar to the result of a calculation of pinning effects in flux flow recently obtained by Yamafuji and Irie[24] for a quite different physical basis and situation.

The essential difficulty is that the pinning points are not independent of each other. Instead they are coupled by the elasticity of the fluxoid lattice. This is demonstrated by considering the effect of a breakaway of a fluxoid from one of the many pinning points with which it interacts along its length. It will relax a little, thus increasing the load on adjacent pinning points and, by its interaction with adjacent fluxoids, increase the load on their pinning points. This cooperative effect has been implicitly introduced in Anderson's and Kim's critical-state concepts by using the "flux bundle" as the pinned entity rather than a single fluxoid.

The importance of these cooperative effects is further illustrated by an argument predicting the total absence of pinning in the limiting case of a perfectly rigid infinite lattice of fluxoids interacting with a perfectly random array of localized pinning potentials of appreciable breadth. Since the rigid lattice could not deform locally for energy minimization, its total energy would be independent of its position with respect to the pinning-point array and there would be no pinning at all.

This discussion suggests that an important parameter is the maximum distance δ that a fluxoid bows out at a pinning point before it is pulled away by the Lorentz force and the forces of interaction with the surrounding

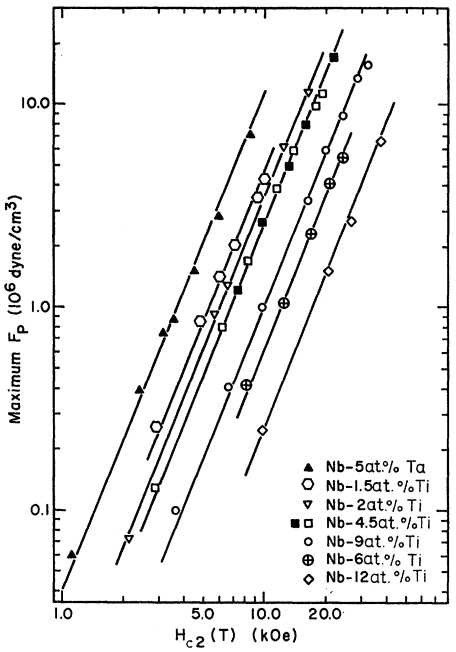

FIG. 11. Logarithmic plot of maximum value of the volume-pinning force F_p(max) as a function of the upper critical field appropriate to the temperature of measurement. Lines with the slope $\frac{5}{2}$ are drawn through the points.

fluxoid lattice. The maximum deformation δ, due to a single pinning point, depends on the strength of the interaction force per pinning point f_1 and the effective stiffness of the fluxoid lattice represented by an elastic constant C times the nominal fluxoid spacing $(\phi_0/B)^{1/2}$. Thus we obtain

$$\delta \approx f_1(a/C)(B/\phi_0)^{1/2}, \tag{6}$$

where a is a constant of order unity. Using[25] $f_1 \approx 10^{-8}$ dyn and $C/a \approx 10^6$ dyn cm^{-2}, we find the extremely small displacement $\delta \approx 10^{-9}$ cm. A similar calculation in the low-field limit using the line energy or tension of a single fluxoid as the restoring force yields essentially the same kind of result. Thus the fluxoid lattice is very rigid and the pinning process must involve a statistical average over all of the interaction forces sampled by this relatively rigid net.

If we assume that the pinning-force density is given simply by a linear superposition of the contribution of all the effective pinning points, we have

$$F_p = f_p N_p, \tag{7}$$

where N_p is an effective density of pinning points and f_p is the maximum pinning force for each interaction.

Assuming that the pinning points consist of individual fluxoid-dislocation interactions, that the fluxoids are relatively stiff, and that their range of interaction with the dislocations is a distance d less than the fluxoid spacing, the effective density of interactions with indi-

[24] K. Yamafugi and F. Irie, Phys. Letters **25A**, 387 (1967).

[25] R. Labusch, Phys. Status Solidi **19**, 715 (1967).

vidual pinning points N_1 is just the product of the length of fluxoid per unit volume B/ϕ_0, the effective area per unit length d, and the density ρ of dislocations threading the area; that is,

$$N_1 \approx (B/\phi_0)\rho d. \tag{8}$$

Typical magnitudes for our cases give $N_1 \approx 10^{11} \times 10^{11} \times 10^{-6} \approx 10^{16}$ cm^{-3}.

As already pointed out, a perfectly rigid lattice interacting with a perfectly random array of localized potentials should accrue no net pinning. However, if the lattice is even slightly deformable, the resulting nonrandom distribution of distances between fluxoids and pinning points gives a net pinning force depending on the distance δ that a fluxoid can be displaced by the pinning potential. In fact, the ratio δ/d, where d is the width of the pinning potential, can be interpreted as the fraction of the points of interaction between fluxoids and obstacles that can become effective in pinning against an applied (Lorentz) force. This result is equivalent to replacing d by δ in Eq. (8). Using Eq. (6), the ratio defines an efficiency factor $W = \delta/d$ as follows:

$$W = (f_p/d)(a/C)(B/\phi_0)^{1/2}, \tag{9}$$

where $f_p = f_1$ is the maximum pinning force of an individual dislocation-fluxoid interaction.

Thus the pinning-force density given by Eq. (7) is simply reduced by the efficiency factor W, giving

$$F_p = f_p N_p W, \tag{10}$$

where W is defined by Eq. (9). Assuming $f_p = f_1$, $N_p = N_1$ as given by Eq. (8) and W as given by Eq. (9), the effective pinning-force density is

$$F_p = f_1^2 \rho (B/\phi_0)^{3/2}(a/C). \tag{11}$$

Thus we find the remarkable result that the pinning-force density is proportional to the square of the strength of individual pinning points because of the appearance of f_1 in the efficiency factor of Eq. (9).

Labusch[6] has carried out a detailed statistical analysis of this many-body problem. His theory indicates that to lowest order in the pinning-point density, $F_p = 0$ unless the quantity that we call an efficiency factor W is greater than unity. This result can be understood as indicating that it is necessary that distortions of the fluxoid lattice must be larger than the width of the pinning potential for pinning to occur; that is, $\delta > d$. However, in our materials with $f_1 \sim 10^{-8}$ dyn and $d \sim 10^{-6}$, we have $\delta \sim 10^{-8}$ and $W \sim 10^{-2}$, so that the expected situation involves only very weak interactions and small fluxoid-lattice distortions.

The above argument indicates a lack of pinning in our case and suggests that the observed pinning might be due to higher-order correlations between pinning points. However, consideration of the effect of fluctuations in the pinning-point distribution leads to pinning by even a random array as a first-order effect as follows: Assuming that only groups of pinning points strong enough that $W \geq 1$ are effective, we seek fluctuations that provide a net local excess of a number of at least n favorable pinning points providing a net strength $f_p \rightarrow f_n \geq n f_1$. The quantity n is determined by the requirement that Eq. (9) yield $W \geq 1$, with $f_p = n f_1$. This configuration should occur with random probability $1/n^2$, so that the effective density of these pinning configurations is $N_p \rightarrow N_n \geq (B/\phi_0)\rho d/n^2$. The criterion that $W \geq 1$ yields

$$n \geq \left[\frac{f_1}{d}\left(\frac{B}{\phi_0}\right)^{1/2}\frac{a}{C}\right]^{-1}. \tag{12}$$

The new values of N_p and f_p can be inserted in Eqs. (9) and (10) to obtain the pinning-force density F_p. However, inserting $N_p = N_n$ and $f_p = f_n$ yields precisely the same pinning strength given by Eq. (11) since n cancels out exactly in the expression for F_p.

Since F_p is independent of n, we can estimate the interaction force f_1 between a single fluxoid and a single dislocation if all other quantities are known. Using the maximum observed value of $F_p \sim 10^7$ dyn cm^{-3} to find the maximum (low-temperature) value of f_1 assuming $\rho = 10^{11}$ cm^{-2}, $B/\phi_0 \approx 10^{11}$ cm^{-2}, and $a/C \approx 10^{-6}$ cm^2/dyn, we find $f_1 \approx 10^{-7}$ dyn which is a factor of 10 larger than the values that have been calculated for a dislocation-fluxoid interaction.[9,10] This number may, however, be overestimated by about one order of magnitude due to uncertainty in f_1 and the probability (to be discussed) that the dislocations are not randomly arranged. Therefore, we think these experiments indicate $10^{-8} < f_1(\max) < 10^{-7}$ dyn.

Ordering of the dislocations into regular arrays should enhance the critical-force density as suggested by Meyerhoff and Heise[26] but we think that the preceding discussion indicates that this is not a necessary condition, contrary to the claim of Narlikar and Dew-Hughes.[27] Nevertheless, pinning is undoubtedly enhanced by the expected clustering of dislocations into the diffuse cell walls known to be characteristic of severe plastic deformation of niobium.[23] Cells about 10^{-4} cm wide with an effective dislocation density $\sim 10^{13}$ cm^{-2} in the walls are expected and would provide clusters containing perhaps $\sim 10^3$ interaction points. This nonrandom distribution of pinning enhances the pinning-force density for a given average dislocation density because the effective pinning force contributed by a cluster increases roughly as the number n in the cell, while the number of these pinning centers decreases roughly as $1/n$ instead of as $1/n^2$ as in the random case.

The collective pinning represented by the pinning force $f_p = n f_1$ in a volume containing between n and n^2 pinning interactions seems to be simply an explicit description of a property of the flux bundle hypothesized

[26] R. W. Meyerhoff and B. H. Heise, J. Appl. Phys. **36**, 139 (1965).

[27] A. V. Narlikar and D. Dew-Hughes, J. Mater. Sci. **1**, 317 (1966).

by Anderson[4] in his original theory of flux creep. The size of this bundle can be estimated from our data, using Eq. (12), which yields $n\sim 10^2$. Thus $n^2=10^4$ and the "bundle volume" $V_p\approx N_p^{-1}n^2\approx n^2/[(B/\phi_0)\rho d]\approx 10^{-12}$ cm^3. From measurements of flux creep in Pb-Tl alloys subjected to severe plastic deformation at low temperatures to produce pinning structures similar to ours, Beasley *et al.*[28] were able to estimate the comparable values of activation volume and energy for pinning of a flux bundle. They observed volumes $\sim 10^4$ times the volume per pinning point and pinning energies $\sim 10^2$ times the energy per pinning point under conditions comparable to ours. This comparison suggests that the cooperative pinning in our analysis of the critical pinning force corresponds to the activation volume or flux bundle invoked to understand flux creep.

It remains to compare the most startling feature of our experimental data—the scaling rules—with the predictions of the model we have presented. The object is to compare the observed temperature and field dependence of the pinning-force density

$$F_p=Kk(\kappa)H_{c2}{}^{5/2}g(B/H_{c2}) \qquad (5')$$

with the calculated pinning-force density which can be written in the form

$$F_p=\rho(H_{c2}/\varphi_0)^{3/2}f_1{}^2(a/C)(B/H_{c2})^{3/2}, \qquad (11')$$

where temperature, field, and κ dependence are implicit in f_1 and a/C.

There are two factors in Eq. (11) that contribute to the temperature dependence of F_p: the fluxoid-lattice elasticity a/C and the pinning force f_1. Labusch[25] has calculated a/C and has given formulas relating the necessary elastic constants of the fluxoid lattice to magnetic properties. In the appropriate limit,[6] we take $a/C=(16\pi C_{66}C_{44})^{-1/2}$, where C_{66} and C_{44} are elastic stiffness constants for the fluxoid lattice given by Labusch. Similar results can be obtained by summation of the forces on a slightly displaced fluxoid due to all other fluxoids using a modified London model due to Coffey[17] without invoking continuum elastic properties of the fluxoid lattice.

The temperature and field dependence of a/C are summarized below for two ranges of B/H_{c2}.

$$a/C=\frac{5\pi^{1/2}\kappa}{(H/B)^{1/2}(B/H_{c2})^{3/2}H_{c2}{}^2}: \quad 0\ll B\ll H_{c2}$$

$$=\frac{0.76}{(B/H_{c2})(1-B/H_{c2})H_{c2}{}^2}: \quad 1-B/H_{c2}\ll 1.$$

At very low fields the "line tension" or self-energy of the fluxoid dominates its deformation, and different statistics may prevail with $F_p\propto f_1{}^{4/3}\rho^{2/3}$ under certain conditions. However, our data are most uncertain in this region and we could not establish evidence for this effect. As $B\to 0$ the effective elastic constant a/C is also not well known. Both the experiments and the model are uncertain in the low-field limit.

There may be several contributions to f_1 for dislocation-fluxoid interactions but the temperature and field contributions for those that can be calculated are quite similar although data needed for accurate determinations are incomplete. We think that the second-order elastic strain perturbation of the condensation energy[9] in the fluxoid core is the dominant pinning contribution so far estimated for this case. It is calculated as the change, as the crystal compliances change at the normal-superconducting transition, of the integral of the dislocation strain energy over the fluxoid volume. One finds $f_1\approx(\Delta S/4)b^2/S^2$, where ΔS is the change of the shear compliance S at the normal to superconducting transition and b is the magnitude of the dislocation burgers vector. At lowest temperatures in niobium, $\Delta S\sim 4\times 10^{-16}$ cm^2/dyn, $S\sim 3\times 10^{12}$ cm^2/dyn, and $b\sim 3\times 10^{-8}$ cm, so that $f_1\sim 10^{-8}$ dyn. The temperature dependence is due to the compliance change which is taken from data on niobium[29] that is consistent with $\Delta S(T)\propto H_c(T)^{3/2}$. The κ dependence is a reasonable guess and the stated temperature dependence may be just an approximation to the sum of a linear and a parabolic term suggested by similarity arguments.[30] The field dependence at high fields is roughly a linear factor of the form $1-B/H_{c2}$ due to the decrease of the maximum of the order parameter between fluxoids. Thus we take

$$f_1\approx\frac{b^2}{4S^2}\Delta S(0)\left(\frac{H_{c2}(T)}{H_c(0)\kappa}\right)^{3/2}\left(1-\frac{B}{H_{c2}}\right)$$

$$\approx 10^{-8}\left(\frac{H_{c2}(T)}{H_c(0)\kappa}\right)^{3/2}\left(1-\frac{B}{H_{c2}}\right).$$

Combining the field, temperature, and κ dependence of all of the factors, we find that the pinning model gives the proportionality

$$F_p\propto H_{c2}(T)^{5/2}$$
$$\times(B/H)/\kappa^2: \quad B \text{ small},$$
$$\times 1/\kappa^2: \quad B\sim H_{c2}/2,$$
$$\times(B/H_{c2})(1-B/H_{c2})/\kappa^3: \quad 1-B/H_{c2}\ll 1, \qquad (13)$$

in satisfactory agreement with our results. The consistency of the properties of this pinning model with our experiments supports its relevance. However, the difficulty of identifying the correct model and pinning mechanisms is illustrated by the fact that the correct functional dependence on B and T can also be obtained from an entirely different pinning model[17] that happens to be inappropriate for the present case.

[28] M. R. Beasley, R. Labusch, and W. W. Webb, Bull. Am. Phys. Soc. **12**, 519 (1967), and (unpublished); see also M. R. Beasley, Materials Science Center Report No. 921, Clark Hall, Cornell University, Ithaca, N. Y. (unpublished).

[29] G. A. Alers and D. L. Waldorf, Phys. Rev. Letters **6**, 677 (1961).

[30] D. P. Seraphim and P. M. Marcus, IBM J. Res. Develop. **6**, 94 (1962).

Better definition of the pinning process due to dislocations would require complete measurements of the elastic coefficients that enter into calculation of the properties of the pinning points,[11] analysis of the dependence of F_p on ρ over a wide range of ρ and dislocation structures, and a systematic analysis of flux creep in the same materials to measure directly the pinning energy and the size of the pinned unit. It is quite likely that the results would prove to be too complex for more than qualitative understanding—like many other properties of dislocations.

Finally, we should consider the evidence for the temperature dependence associated with thermal activation of flux motion. Equation (4) has two terms and the linear temperature dependence associated with thermal activation is represented by the second term. Only if $k_BT\ln(R_0/R_c)\gtrsim U_p$ will the effects of thermal activation be observable. The lowest reasonable value of $U_p\approx f_pd$ seems to be $\sim10^{-8}\times10^{-6}\sim10^{-14}$ erg and the largest value of $k_BT\ln(R_0/R_c)$ is $<10^{-15}$. Therefore, the linear term in T is not ordinarily detectable and the simplifying heuristic assumption $F_p\cong F_c$ that we used in the present case is justified. Thus the temperature dependence of the critical current is due entirely to the temperature dependence of the pinning-point strength and the fluxoid-lattice stiffness and *not* to a term in k_BT due to thermal activation. Although flux creep does occur, its effect on the measured critical state is small. We have already mentioned that the activation volume or flux-bundle volume and the effective pinning energy found by Beasley *et al.*[28] from flux-creep measurements on alloys with similar pinning structures are similar to the pinning energies deduced from our critical pinning-force measurements. We found at lowest temperatures a pinning energy $U_p\approx10^{-12}$ erg and $V_p\sim10^{-12}$ cm^3. The comparison can be carried further by considering the high-field limit. As $B\rightarrow H_{c2}$, both U_p and f_p vanish and this result is reflected in both creep and critical pinning-force measurements. The activation volume for flux creep has been observed to decrease to a nonzero limit as $B\rightarrow H_{c2}$. A nonzero temperature-dependent minimum bundle volume is also predicted by our pinning model.

ACKNOWLEDGMENTS

We are grateful to Dr. R. Labusch for many helpful conversations and for explanation of his statistical model of fluxoid-lattice pinning. Finally one of us (W. W. W.) thanks Professor W. A. Little and the Physics Department at Stanford University for their hospitality while this manuscript was being completed.

APPENDIX: MAGNETIC MOMENT OF A HYSTERETIC CYLINDRICAL SPECIMEN

A long cylinder of reversible type-II superconductor with negligible demagnetizing factor in a uniform applied magnetic field H_a directed along the axis of the cylinder should show uniform magnetic induction, $B(H_a)=H_a+4\pi M_e(H_a)$, where $M_e(H_a)$ is the equilibrium magnetization of the specimen in applied field H_a.

However, if flux-pinning sites are present within the material, B is generally not uniform but is an irreversible but well-defined function of the past magnetic history of the specimen if a boundary condition, the value of B just inside the surface, can be specified for all values of applied field H_a. A simple model for the hysteretic material is obtained by assuming that this boundary value of magnetic induction B_0 is a single-valued function of the applied field and is just equal to $H_a+4\pi M_e(H_a)$. This assumption neglects surface hysteresis effects and supposes that pinning sites may be introduced without altering the basic superconducting parameters of the material. Both of these assumptions appear to valid for reasonably high values of κ at $0.2H_{c2}<B<0.9H_{c2}$.

With these boundary conditions and the assumption that a critical state, defined by a critical current $J_c(B,T)$, exists throughout the specimen, a simple result can be obtained relating the magnetic moment at an applied field H_a to the critical current density $J_c(B,T)$ evaluated at a value of B equal to the boundary field B_0. Thus we obtain values for the function $J_c(B,T)$ by varying B_0 over a suitable range of values.

Suppose the magnetic induction $B(r)$ existing in a cylindrical specimen at an applied field H_a is everywhere greater than zero, extends smoothly to the center, and has the boundary value $B(R)=B_0$, where R is the radius of the specimen. There are two possible field configurations consistent with these restrictions and the critical-state model, shown in Fig. 12 and labeled $B_+(r)$ and $B_-(r)$. These are the configurations expected from smoothly sweeping the applied field either up to or down to H_a from zero or from a value above H_{c2}. The associated critical current configurations are $J_+(B_+)$ and $J_-(B_-)$, which may be considered as functions of the radius r with a parametric dependence on the boundary field B_0. For the conditions specified above, it is possible to expand the currents in a Taylor series about the point $r=R$, so that

$$J_+(r)=J_+(R)+J_+'(R)(r-R)+J_+''(R)(r-R)^2/2!+\cdots \quad \text{(A1)}$$

and

$$J_-(r)=J_-(R)+J_-'(R)(r-R)+J_-''(R)(r-R)^2/2!+\cdots, \quad \text{(A2)}$$

where the primes indicate derivatives with respect to r.

The induction B for the two cases is obtained by integrating the series above, giving

$$B_+(r)=B_0+k[J_+(R)(r-R)+J_+'(R)(r-R)^2/2!+\cdots] \quad \text{(A3)}$$

and

$$B_-(r)=B_0+k[J_-(R)(r-R)+J_-'(R)(r-R)^2/2!+\cdots], \quad \text{(A4)}$$

where $k=4\pi/10$ if J is in amperes per square centimeter and B is in gauss.

Finally the magnetic moment, defined in terms of an average magnetization $\bar{M}$, is obtained by performing the integration

$$4\pi\bar{M}=\frac{1}{\pi R^2}\int_0^{2\pi}d\theta\int_0^{2\pi}[B(r)-H_a]rdr, \quad \text{(A5)}$$

which, with the assumption that $B_0=H_a+4\pi M_e$, yields

$$4\pi\bar{M}_+=4\pi M_e+2k\left(\frac{J_+R}{3!}-\frac{J_+'R^2}{4!}+\frac{J_+'R^3}{5!}-\cdots\right) \quad \text{(A6)}$$

and

$$4\pi\bar{M}_-=4\pi M_e+2k\left(\frac{J_-R}{3!}-\frac{J_-'R^2}{4!}+\frac{J_-''R^3}{5!}-\cdots\right), \quad \text{(A7)}$$

where all derivatives of J_+ and J_- are evaluated at the surface.

Now the critical-state model assumes a relationship between the magnitude of the critical current and the local field; hence

$$|J_c(B)|=|J_+(B)|=|J_-(B)|. \quad \text{(A8)}$$

It can be shown that

$$\partial^n J_+/\partial r^n=(-1)^n\partial^n J_-/\partial r^n \quad \text{at} \quad r=R. \quad \text{(A9)}$$

Thus the two series given above for $\bar{M}_+$ and $\bar{M}_-$ have terms that are equal in magnitude but the odd terms have opposite signs. Their difference is

$$4\pi(\bar{M}_+-\bar{M})=\frac{2kJ_+R}{3}+\frac{4kJ_+''R^3}{5!}+\cdots, \quad \text{(A10)}$$

and their sum is

$$4\pi(\bar{M}_++\bar{M}_-)=2(4\pi M_e)-\frac{kJ_+R^2}{3!}+\cdots, \quad \text{(A11)}$$

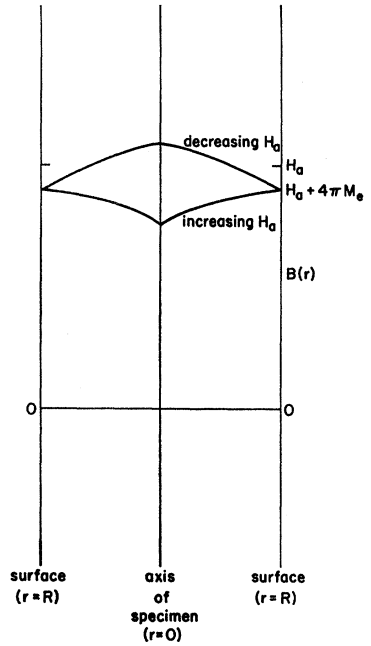

FIG. 12. Assumed schematic magnetic field distribution within the worked specimen. Only these two configurations are consistent with the critical-state model and the assumptions of the text. These represent the two branches of the hysteretic magnetization loop described in the Appendix.

a result similar to that previously obtained for a flat-plate geometry[3] assuming a particular form for $J_c(B)$. In regions where the series converge rapidly, the simple results

$$4\pi(\bar{M}_+-\bar{M}_-)\approx\tfrac{2}{3}kJ_cR \quad \text{(A12)}$$

and

$$4\pi(\bar{M}_++\bar{M}_-)\approx 2(4\pi M_e) \quad \text{(A13)}$$

are obtained, from which $J_c(B)$ and $4\pi M_e(H_a)$ can be calculated.